Dynamics of single vortices in grain boundaries: I - V characteristics on the femtovolt scale

B. Kalisky, J. R. Kirtley, E. A. Nowadnick, R. B. Dinner, E. Zeldov, Ariando, S. Wenderich, H. Hilgenkamp, D. M. Feldmann, and K. A. Moler

---

Articles you may be interested in

Evaluation of vortex pinning across low angle grain boundary in YBa2Cu3O7 film
Appl. Phys. Lett. **101**, 112604 (2012); 10.1063/1.4752462

Enhanced current flow through meandering grain boundaries in Y Ba 2 Cu 3 O 7 − δ films
Appl. Phys. Lett. **90**, 212501 (2007); 10.1063/1.2740610

Combined effect of a single grain boundary and artificial pinning centers on the critical current density in a Y Ba 2 Cu 3 O 7 − δ thin film
Appl. Phys. Lett. **89**, 172505 (2006); 10.1063/1.2364186

Correlation between grain and grain-boundary critical current densities in ex situ coated conductors with variable YBa 2 Cu 3 O 7 − δ layer thickness
Appl. Phys. Lett. **88**, 122502 (2006); 10.1063/1.2188044

Direct detection of the magnetic flux noise from moving vortices in wide YBa 2 Cu 3 O 7−δ grain boundary junctions
Appl. Phys. Lett. **78**, 1715 (2001); 10.1063/1.1355669

Dynamics of single vortices in grain boundaries: *I-V* characteristics on the femtovolt scale

B. Kalisky,[1,a)] J. R. Kirtley,[1] E. A. Nowadnick,[1] R. B. Dinner,[1,b)] E. Zeldov,[1,2] Ariando,[3,c)] S. Wenderich,[3] H. Hilgenkamp,[3] D. M. Feldmann,[4] and K. A. Moler[1]

[1]*Geballe Laboratory for Advanced Materials, Stanford University, Stanford, California 94305, USA*
[2]*Department of Condensed Matter Physics, Weizmann Institute of Science, Rehovot 76100, Israel*
[3]*Low Temperature Division, Mesa+ Institute for Nanotechnology, University of Twente, P.O. Box 217, 7500 AE Enschede, The Netherlands*
[4]*Los Alamos National Laboratory, Los Alamos, New Mexico 87545, USA*

We employed a scanning Hall probe microscope to detect the hopping of individual vortices between pinning sites along grain boundaries in YBa$_2$Cu$_3$O$_{6+\delta}$ thin films in the presence of an applied current. Detecting the motion of individual vortices allowed us to probe the current-voltage (*I-V*) characteristics of the grain boundary with voltage sensitivity below a femtovolt. We find a very sharp onset of dissipation with $V \propto I^n$ with an unprecedented high exponent of $n \approx 290$ that shows essentially no dependence on temperature or grain boundary angle. Our data have no straightforward explanation within the existing grain boundary transport models. © *2009 American Institute of Physics*. [DOI: 10.1063/1.3137164]

Grain boundaries (GBs) in high-T_C superconductors,[1] widely used for devices and fundamental studies,[2,3] govern the transport properties of many superconductors with technological applications.[4] It is therefore important to understand the mechanism for dissipation in transport across GBs. GB transport is usually studied with such a large voltage threshold (nanovolts) that millions of vortices traverse the boundary per second. Although not on a grain boundary, effective voltage thresholds of picovolts using a superconducting quantum interference device volt meter[5] and noise spectral densities of milliattovolts from flux noise in superconducting rings[6] have been reported. Extremely small effective voltages have been inferred from measurements of flux relaxation in superconducting rings.[7,8] Here, we report direct imaging of GBs in YBa$_2$Cu$_3$O$_{6+\delta}$ with a scanning Hall probe microscope.[9] By sensing individual vortices, we demonstrate an effective voltage threshold of 0.2 fV and quantitatively measure dissipation with an onset threshold of attowatts. The results are striking: the frequency of vortex motion increases exponentially with current above a threshold current, but the exponent does not depend strongly on either temperature or grain boundary misorientation angle. We compare our data to models of vortex motion in grain boundaries,[1,10–16] and surprisingly find that none of the existing models can fully describe the data.

The data shown here are from a 250 nm thin film of YBa$_2$Cu$_3$O$_{6+\delta}$ ($T_C = 89.5$ K), epitaxially grown by pulsed laser deposition on a substrate of symmetric 24° [001] tilt oriented bicrystal of SrTiO$_3$. 21 bridges with widths of 20, 50, and 100 μm were patterned with the GB perpendicular to the bridge [Fig. 1(a)]. We also measured a 50 μm wide bridge patterned from a 180 nm thin film on a 5° [001] bicrystal. Magnetic measurements were performed with a large-area scanning Hall probe microscope,[9] with single vortex resolution and a 10 kHz bandwidth. The magnetic resolution is 4 mG/$\sqrt{\text{Hz}}$ and the spatial resolution in the data presented is ≥ 1 μm: pixel size is 200 nm, and the data shown were taken with a 1×1 μm^2 Hall cross 1 μm from the surface. Four-probe transport measurements of the sample were made with a voltage noise floor of 1 μV.

Large angle GBs with critical currents much lower than the surrounding grains[1,12,14] provide a well defined narrow channel for vortex motion. Figure 1(b) shows a magnetic image of a 50 μm wide GB, at $T = 10$ K, with applied current I larger than its critical current. Single vortices, observed in the bulk due to cooling in an ambient field of ~ 0.15 G, are well pinned at this applied current. On the GB, however, vortices move continuously from both edges toward the central (white) region. A fit of this image using the monopole model for each single vortex, with the vortex positions as free parameters, finds 10 negative (blue) and 23 positive (red) vortices on the GB, unevenly spaced with a minimum separation of 1 μm. When the applied current is turned off, many vortices stay trapped on the GB. However, after thermal cycling we can image single vortices on the GB, as shown in Fig. 1(c). Bulk and GB vortices look the same with our spatial resolution, indicating $\lambda_{GB} \leq 1$ μm.

Figure 2 shows a pseudocolor image of the noise spectra for different I at location 1 indicated in Fig. 1(b). The low-frequency noise increases dramatically when the applied current exceeds a temperature dependent threshold value I_{th}. The spectrum broadens rapidly with further current increase. Similar behavior was observed at different locations along the GB but disappeared in 2–3 μm away from the GB. The excess noise location on the GB and its dependence on sample current relate it to the dynamics of vortices in the one-dimensional (1D) channel of the GB.

The noise spectrum has a Lorentzian shape (inset of Fig. 2) consistent with a two-level random telegraph noise,[17,18] implying a random hopping of vortices along the GB, rather than a smooth correlated motion. The shift of the Lorentzian

a)Electronic mail: beena@stanford.edu.
b)Present address: Department of Materials Science, Cambridge University, United Kingdom.
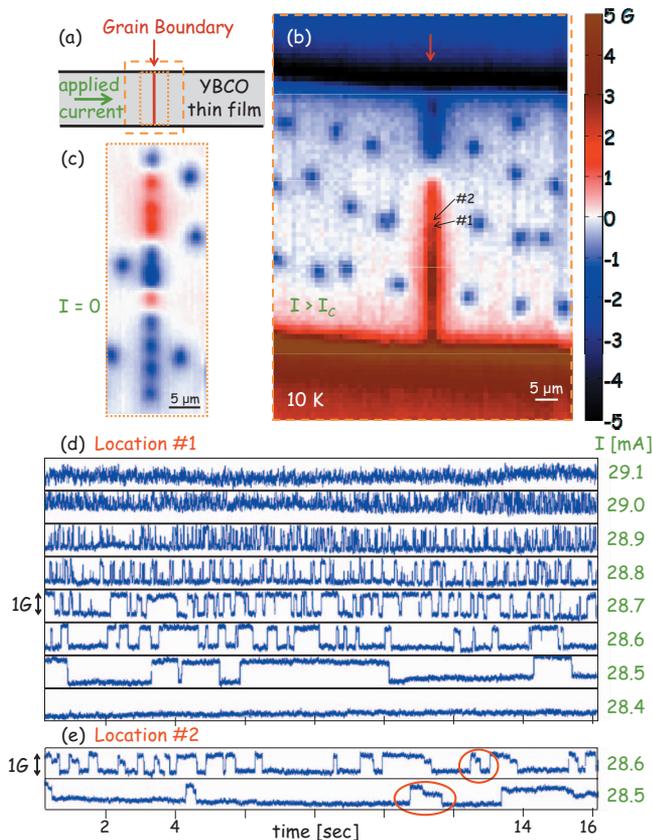c)Present address: Department of Physics, National University of Singapore, Singapore.

FIG. 1. (Color) (a) Sketch of the GB sample. The bridge width is 50 μm, GB misorientation angle is 24° symmetric (*a* and *b* axes are −12° and 12° with respect to the GB). [(b) and (c)] Magnetic image of the GB area (b) at 10 K and $I=29$ mA and (c) at 10 K and $I=0$, showing individual vortices (red) and antivortices (blue). The regions imaged are marked by the orange frames in (a). [(d) and (e)] The Hall probe signals vs time at 10 K for different currents applied to the GB measured at two positions marked in (b). The switching events are vortices passing under the probe. Red circles indicate three-level switching events.

to higher frequencies with increasing current shows that the vortices hop faster with increasing Lorentz force as expected. At each current above I_{th}, the total value of the excess noise (difference between the integrals of the power spectral density above and below I_{th}) remains rather constant and matches the peak value measured for a single vortex by the static imaging ($\sim$1 G).

The motion of vortices is also apparent in the time resolved Hall probe signal. Figures 1(d) and 1(e) show time traces at two locations along the GB marked in Fig. 1(b), recorded for 16 s (3×10^5 data points) at each I with 60 Hz background noise (see Fig. 2) filtered out. For $I<28.5$ mA no vortex motion was detected as seen in the corresponding trace in Fig. 1(d). At 28.5 mA individual rare switching events become visible, with the amplitude of a single vortex. The rate of switching events increases with increasing current. Above a certain current the vortex rate exceeds our bandwidth. No correlation was observed between events, which implies random vortex hopping between pinning sites. At different locations along the GB, different types of signals were observed—positive vortices (in the red region), negative vortices (blue region), and a mixture of the two close to the annihilation region. Also, in some cases three- or four-level signals were observed at certain locations along the GB, which can be explained by the presence of a few pinning sites in close proximity to the Hall sensor. An example
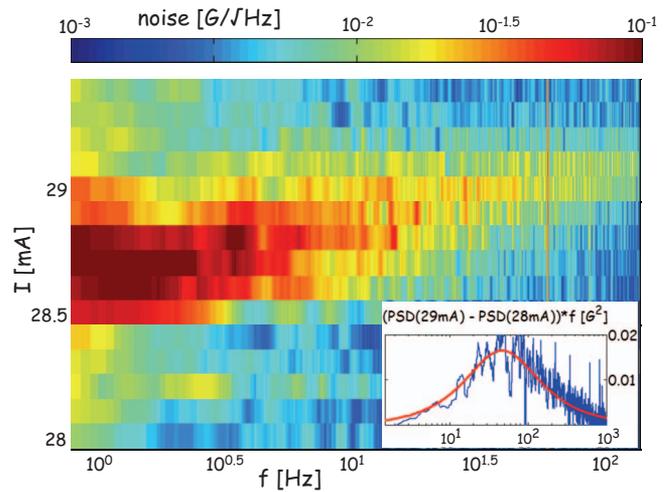

FIG. 2. (Color) Pseudocolor image of the noise spectrum of the Hall signal for different sample currents at 10 K, measured at the location 1 in Fig. 1(b). Inset: difference between the power spectral densities at currents of 29 and 28 mA (green). The Lorentzian shaped spectrum is multiplied by f similarly to the analysis in Ref. 16. The fit to two-level random telegraph noise is plotted in red.

of a three-level signal is shown in Fig. 1(e), recorded at 10 K at location 2 in Fig. 1(b) (1 μm away from location 1). We interpret the sequences circled in Fig. 1(e) as representing a vortex moving from a site directly under the Hall bar, to one close to, but not directly under it, to a site far from the Hall bar. Such signals were more frequently observed at the higher temperature of 50 K, possibly because vortices are larger and overlap more. At this site, the highest level always precedes the intermediate level, indicating that the vortices are moving in one direction.

As the vortex motion appears to be in one direction, we assume that each vortex hopping event corresponds to a vortex crossing the entire grain boundary, and we can therefore extract the I-V characteristics using the Josephson relation $V=\Phi_0 f$, where Φ_0 is the flux quantum. The rate of passing vortices f, was measured either by counting vortices on the time traces [e.g., Figs. 1(d) and 1(e)] or by fitting the noise spectrum (Fig. 2) to a Lorentzian. Figure 3 shows I-V curves at 10 K (red) and 50 K (blue). The current axis is normalized by $I_{th}(10\ K)=28.5$ mA, the lowest current at which vortices
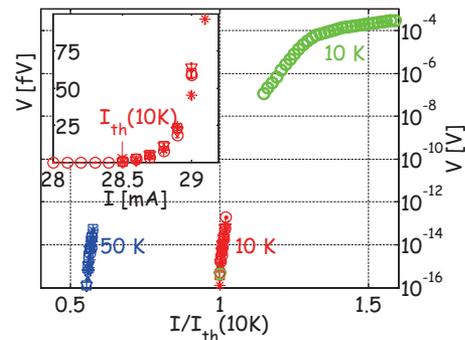

FIG. 3. (Color) Current-voltage characteristics. The low voltage part (red and blue) was measured magnetically by the Hall probe [as shown in Figs. 1(d) and 2]. Different symbols are different locations along the GB. The current axis is normalized by $I_{th}(10\ K)$ which is the lowest current at which vortices were observed moving at 10 K. The high voltage part (green) was acquired by four-probe measurements on a neighboring bridge with identical dimensions and normalized to I_{th} of that bridge measured magnetically (green data on the low voltage part). Inset: low voltage data at 10 K on a linear scale.

were observed moving at 10 K. Such "magnetic" measurements of the voltage on a single vortex scale allow 0.2 fV sensitivity, where the average rate of passing vortices is ~ 0.1 Hz.

The onset of dissipation is quite steep: at 10 K V changes by three orders of magnitude as I changes by $\delta I/I = 0.03$, and at 50 K $\delta I/I = 0.037$. The low voltage part of I-V can be equally well fitted by power law $V \propto I^n$ or exponential behavior $V \propto \exp(mI/I_c)$, where m, n, and I_c are fitting parameters. For both, the characteristic exponent is very high, $n \approx m \approx 290$, and independent of T in the measured range of 10–50 K. For the $5°$ grain boundary at 40 K we find $\delta I/I = 0.04$. In all our measurements, $\delta I/I$ was between 0.03 and 0.05. Note that although the exponent is not T dependent, the critical current, at which dissipation starts, decreases with T as expected[10,14] since the gap and order parameters are decreasing. At higher voltages, conventional four-probe measurements are shown by green data points.[19] The shape of the high voltage part is similar to I-V curves observed in the literature.[1,12,14] For three of our $24°$ GB we found $I_c R_n$ products of 0.93, 1.68, and 0.94 mV at 10 K, and our $5°$ GBJ had an $I_c R_n$ product of 0.4 mV at 40 K. At 86 K the current-voltage characteristics had little hysteresis, consistent with our estimate of $\beta_c = 2\pi I_c R_n^2 C/\Phi_0 < 1$.

The Hall probe's possible perturbation of the sample should not be important. The magnetic field generated by the Hall probe is about 0.03 G, too small to affect the vortex dynamics. The tip of the Hall probe chip touching the sample may exert an applied force (~ 1 μN) and local heating (~ 10 μW).[9] The onset current for vortex motion changes slightly with the Hall probe's distance from the grain boundary, consistent with a local temperature rise of ~ 0.2 K, but the shape and quantitative slope of the I-V curve remain the same. The magnetic signal varies with position perpendicular to the GB like a single vortex does, as expected for a 1D channel. The noise data is consistent with the I-V measurements, in that a relatively smooth curve can be drawn between the two sets of data (see Fig. 3).

Several scenarios were considered to explain the experimental observations:

(i) The shape of the I-V curves, the range of T, and the observed hopping all demonstrate the importance of pinning sites and suggest *creep* behavior. We considered several pinning potential shapes.[20,21] Although some predict an I-V shape that resembles the data, all also predict a temperature dependent exponent inconsistent with our data. Also, the large exponent n observed implies that the barrier is much larger than thermal fluctuations over the entire range of 10–50 K. Such a large n has not been reported in the literature.

(ii) For our $24°$ GB, Josephson vortices or *Abrikosov–Josephson vortices*[13,18,20] are expected. For the latter, a nonlinear *flux flow* behavior is expected, due to the expansion of the vortex Josephson-core from ξ to λ as the current is increased.[22] Our measurements are performed in a range where the presence of Abrikosov–Josephson vortices is very likely.[15,22] However, this scenario cannot explain the T independence of the exponent.

(iii) The presence of pinning, the steep curvature of the I-V and its decrease at higher voltages suggest a *glassy*

behavior[20,23] with exponential I-V which can describe our data. However, care should be taken in relating this model to our case, which deals with 1D motion of vortices that are flat (250 nm) and relatively sparse. Also, the lack of T dependence of the exponent remains a problem.

(iv) The lack of T dependence, and the very large pinning barrier relative to thermal fluctuations suggest the possibility of *quantum tunneling* of vortices. An estimate of the quantum tunneling rate of Josephson vortices in our GB geometry can be made to fit our experiments (see supplementary material[24]). However, unrealistically high values for the attempt frequency and low values for the junction capacitance are required for these fits.

In summary, the dynamics of vortices on GBs were measured in the limit of extremely low dissipation. The vortices hop between pinning sites with a characteristic frequency that depends on the applied current. I-V characteristics were extracted, with voltage sensitivity as good as 2×10^{-16} V. At low voltages the I-V curves are very steep with temperature independent exponents. Our data are qualitatively different from grain-boundary transport measurements at higher voltages,[1,12,14] and cannot be fully explained using existing models.

[1]H. Hilgenkamp and J. Mannhart, Rev. Mod. Phys. **74**, 485 (2002).

[2]C. C. Tsuei *et al.*, Phys. Rev. Lett. **73**, 593 (1994).

[3]C. C. Tsuei and J. R. Kirtley, Rev. Mod. Phys. **72**, 969 (2000).

[4]J. Mannhart and P. Chaudhari, Phys. Today **54**, 48 (2001).

[5]H. Safar *et al.*, Phys. Rev. Lett. **68**, 2672 (1992).

[6]F. C. Wellstood *et al.*, Phys. Rev. Lett. **70**, 89 (1993).

[7]E. Sandvold and C. Rossel, Physica C **190**, 309 (1992).

[8]I. L. Landau and H. R. Ott, Physica C **340**, 251 (2000).

[9]R. B. Dinner, M. R. Beasley, and K. A. Moler, Rev. Sci. Instrum. **76**, 103702 (2005).

[10]J. Mannhart *et al.*, Phys. Rev. Lett. **61**, 2476 (1988).

[11]D. Winkler *et al.*, Phys. Rev. Lett. **72**, 1260 (1994).

[12]N. F. Heinig *et al.*, Phys. Rev. B **60**, 1409 (1999).

[13]A. Diaz *et al.*, Phys. Rev. B **58**, R2960 (1998).

[14]D. Dimos, P. Chaudhari, and J. Mannhart, Phys. Rev. B **41**, 4038 (1990).

[15]A. Gurevich *et al.*, Phys. Rev. Lett. **88**, 097001 (2002).

[16]R. D. Redwing *et al.*, Appl. Phys. Lett. **75**, 3171 (1999).

[17]S. J. Machlup, J. Appl. Phys. **25**, 341 (1954).

[18]J. R. Kirtley *et al.*, J. Appl. Phys. **63**, 1541 (1988).

[19]Four-probe transport measurements were acquired on a neighboring bridge with identical dimensions and normalized to I_{th} of that bridge, 34 m A at 10 K, measured with Hall probe.

[20]G. Blatter *et al.*, Rev. Mod. Phys. **66**, 1125 (1994).

[21]E. Zeldov *et al.*, Appl. Phys. Lett. **56**, 1700 (1990).

[22]A. Gurevich, Phys. Rev. B **65**, 214531 (2002).

[23]D. S. Fisher, M. P. A. Fisher, and D. A. Huse, Phys. Rev. B **43**, 130 (1991).

[24]See EPAPS Document No. E-APPLAB-94-038920 for a file that describes an estimation of the quantum tunneling rate of Josephson vortices in our GB geometry. For more information on EPAPS, see http://www.aip.org/pubservs/epaps.html.